NJC

Accepted Manuscript

This is an *Accepted Manuscript*, which has been through the Royal Society of Chemistry peer review process and has been accepted for publication.

Accepted Manuscripts are published online shortly after acceptance, before technical editing, formatting and proof reading. Using this free service, authors can make their results available to the community, in citable form, before we publish the edited article. We will replace this *Accepted Manuscript* with the edited and formatted *Advance Article* as soon as it is available.

You can find more information about *Accepted Manuscripts* in the Information for Authors.

Please note that technical editing may introduce minor changes to the text and/or graphics, which may alter content. The journal's standard Terms & Conditions and the Ethical guidelines still apply. In no event shall the Royal Society of Chemistry be held responsible for any errors or omissions in this *Accepted Manuscript* or any consequences arising from the use of any information it contains.

ROYAL SOCIETY OF CHEMISTRY

www.rsc.org/njc

Cite this: DOI: 10.1039/c0xx00000x

www.rsc.org/xxxxxx

ARTICLE TYPE

Glutathione-directed synthesis of Cr(VI)- and temperature-responsive fluorescent copper nanoclusters and their applications in cellular imaging

Lingcan Kong,[a*] Xuefeng Chu,[b] Wenwei Liu,[a] Yuyang Yao,[a] Pengfei Zhu[a] and Xia Ling[a*]

Received (in XXX, XXX) Xth XXXXXXXXX 20XX, Accepted Xth XXXXXXXXX 20XX

DOI: 10.1039/b000000x

Water-soluble and highly fluorescent copper nanoclusters (Cu NCs) using glutathione as a stabilizing agent have been prepared. The as-prepared Cu NCs have an average diameter of about 2.2 nm and are shown to be viable fluorescent probe for the determination of Cr(VI) ion owing to the inner filter effect of Cr(VI) ion. The Cu NCs have been characterized in terms of photoluminescence excitation spectrum, photoluminescence spectrum, transmission electron microscopy, Fourier transform infrared spectroscopy (FT-IR), and X-ray photoelectron spectroscopy. Furthermore, the nanosensor exhibits high sensitivity to Cr(VI) ion with a detection limit of 1.5 μM and has been demonstrated for determination of Cr(VI) ion in real water samples including tap water, mineral water, and Taihu lake water. In addition, the as-prepared NCs could be used as versatile nanothermometry devices in cellular and in vivo temperature sensing based on obvious temperature dependence on the fluorescence emission intensity, which changes obviously over physiological temperature range (279 K–323 K).

Introduction

Heavy metal ions, such as Hg^{2+}, Pb^{2+}, Cu^{2+}, could result in permanent damage to human health owing to their accumulative characters in the environment and biota.[1–3] Among them, chromium ion has received much attention because it has been extensively used in various industrial processes and has become one of the major environmental hazards.[4] The toxicological and biological properties of chromium are entirely dependent on its electric charge.[5] For example, Cr(VI) ion is extremely harmful to the biosphere and is known to be a strong carcinogen; even trace amounts could pose a detrimental risk to human health.[6] In contrast, Cr(III) ion is relative non-toxic and is regarded as an essential element associated with biological processes.[7] Thus, the reduction of Cr(VI) ion to Cr(III) ion is a critical process for detoxification in the Cr-contaminated water. The World Health Organization proposes a guideline limit of 0.04 $mg \cdot L^{-1}$ for chromium in drinking water.[8] Therefore, the detection of trace levels of Cr(VI) in contaminated water is an important topic.[9]

On the other hand, temperature is one of the most important physical factors which plays an important role in temperature-dependent systems such as environment and physiological processes.[10] The accurate measure of it is tremendous significance owing to its widespread use in medical diagnostics and electronic devices.[11] Up to now, numerous temperature sensors have been developed and widely applied in environmental temperature measurement, biomedical sensing, and thermal monitoring of microprocessors.[12] Among them, fluorescence-based temperature sensing is a versatile technique to monitor the local temperature due to their high resolution and fast responses.[13] Indeed, several fluorescent nanomaterials including organic dyes, quantum dots, inorganic phosphors have been employed for temperature detection, which operates by temperature-dependent emission intensity changes.[14–16] Moreover, fluorescent metal NCs have already shown great potential for temperature sensor in biological and live cells.[17] However, the complicated synthesis, toxicity, and expensive price make some materials unsuitable for many practical application.[18] Thus, an excellent probe should be not only highly sensitive and selective but also simple, safe, and economical simultaneously.

Metal clusters are interesting classes of materials that are known to be isolated particles with several to tens of metal ions and size comparable to the Fermi wavelength of electrons.[19] Owing to their molecular-like electron transitions and intense fluorescence, NCs materials has been extensively studied for their widely potential applications in bioimaging, biosensing, catalysts, and various other applications.[20–23] Similar to quantum dots, metal NCs show size-dependence tunable fluorescence from visible to near infrared regions with high quantum yields.[24] Biomolecule-conjugated fluorescent metal NCs have been considered as a powerful technique for the detection of low concentration analytes due to their facile synthesis, low cost, excellent biocompatibility, and multifunctional surface chemistry.[25] For example, Zhang and coworkers reported Au/Ag alloy NCs for highly selective detection of Pb^{2+} ion at ppb level.[26] Wang and coworkers used red fluorescent gold NCs as effective probe for the detection of Ag^{+} ion.[27] Although there are a number of reports on the detection of low concentration analytes by using fluorescent NCs,[28] corresponding studies on nanothermometers by using metal NCs are very rare.[29]

Inner filter effect (IFE) is one sensing mechanism used to design fluorescence probes for detection of metals, which needs a good spectral overlap between the absorption band of the absorber (such as metal ion) and the excitation band and/or emission band of the fluorophore.[9] Compared with other

mechanisms, such as photo-induced electron transfer, fluorescent resonance energy transfer, and metal-ligand charge transfer, IFE has great advantages including simplicity, convenience, and rapid implementation.[30] However, a rare Cu NCs-based nanosensor was developed via inner filter effect. Therefore, it is envisaged that the combination of intense fluorescence properties of Cu NCs and water-soluble as well as biocompatible characters of glutathione moiety together with the detection of low concentration ions based on inner filter effect and nanothermometry devices over the physiological temperature range may provide attractive multifunctional features for the development of multifunctional materials. This will allow the systematic study of the influence of ion/temperature on Cu NCs protected by glutathione, which will provide important insights into the future design of multifunctional materials. Herein is described the synthesis of fluorescent Cu NCs with protection by glutathione. Glutathione could significantly restrict the size of Cu NCs during the nucleation and growth processes, and prevent NCs from becoming large nanoparticles.[31] In addition, abundant functional groups including thiols, carboxyl, and amino groups make fluorescent Cu NCs exhibit good dispersion and high stability in water.[32] These advantages suggest that the resultant Cu NCs are promising fluorescent probes for detection of ions and cellular temperature sensing in aqueous solution.

Experimental

Materials

Reduced glutathione (GSH, molecular weight of 307 $g \cdot mol^{-1}$) was purchased from Aldrich. Copper sulphate ($CuSO_4$), copper nitrate ($Cu(NO_3)_2$), copper chloride ($CuCl_2$), copper acetate ($Cu(AcO)_2$), hydrazine hydrate ($NH_2NH_2 \cdot H_2O$), isopropanol were analytical grade. All reagents were used as received without further purification. De-ionized water was used in all experiments.

Preparation of water-soluble fluorescent Cu NCs

The Cu NCs were prepared as previously reported with a slight modification.[24] 80 mg of glutathione and 7 mg copper sulphate were dissolved in de-ionized water (5 mL) and supramolecular hydrogel was formed. After hydrazine hydrate (1 mL) was diluted to 25 times with water (25 mL), 400 µL hydrazine hydrate was added to the above mixture and transparent solution was obtained. The Cu NCs were obtained upon addition of isopropanol, centrifuged at 10,000 rpm to remove the solvent and redispersed in de-ionized water for further application.

Application as Cr(VI) Probe

Stock solution of $K_2Cr_2O_7$ with the concentration of 8 $mmol \cdot L^{-1}$ was prepared and various $Cr_2O_7^{2-}$ concentrations were diluted by serial dilution at room temperature. To check the selectivity of the Cu NCs, other ions including cation ions (Na^+, Ba^{2+}, Cd^{2+}, Cu^{2+}, Co^{2+}, Fe^{3+}, Hg^{2+}, Mg^{2+}, Mn^{2+}, Zn^{2+}, Pb^{2+}, Ag^+, Fe^{2+}, Al^{3+}, Cr^{3+}), anion ions (F^-, Cl^-, Br^-, I^-, CN^-, BrO_3^-, $S_2O_8^{2-}$, SCN^-, MnO_4^-), and H_2O_2 were carried out. All the experiments were similar as performing for the detection of Cr(VI) ion.

Characterization methods

UV-Vis absorbance spectra were recorded on a Cary 50 scan spectrophotometer at room temperature. The fluorescence spectra were recorded by using a Shimadzu RF-5301 spectrofluorimeter. TEM imaging were obtained with a JEM-2100F transmission electron microscope (TEM) operating at 200 kV. X-ray photoelectron spectroscopy is obtained in a VG ESCALAB MKII spectrometer using Mg K_α excitation (1253.6 eV) and bind energy calibration is based on C 1s at 284.6 eV. The Fourier transform infrared spectroscopy was measured at wavenumbers ranging from 500 cm^{-1} to 4000 cm^{-1} using a Nicolet Avatar 360 FT-IR spectrophotometer. The confocal microscopy images were taken using an Olympus Fluoview FV1000.

Cellular imaging

The HeLa cells were cultured in Dulbecco's modified Eagle's medium supplemented with 10% fetal bovine serum and 1% penicillin/streptomycin (DMEM) using a 96-well plate. Suspensions (20 $\mu g \cdot mL^{-1}$) of GSH-Cu NCs from the stock solution were prepared with Dulbecco's phosphate buffer saline (DPBS). After sonication for 10 min to ensure complete dispersion, an aliquot (typically 0.01 mL) of the suspension was added to the well of a chamber slide, then incubated at 310 K in a 5% CO_2 incubator for 24 h. Prior to fixation of the HeLa cells on the slide for inspection with a confocal fluorescence microscope, the excess GSH-Cu NCs were removed by washing 3 times with warm DPBS.

Result and discussion

Synthesis of fluorescent Cu NCs

The process of glutathione-directed synthesis of stable, water-soluble, and fluorescent copper Cu NCs is shown in Scheme 1. In a typical experiment, glutathione and copper sulphate were dissolved in de-ionized water and supramolecular gel was formed owing to the interaction between copper ion and glutathione with similar results reported in the previous literatures.[19] After that, diluted $N_2H_4 \cdot H_2O$ was added to the above mixture, the supramolecular gel disappeared and transparent solution was obtained. Subsequently, the solution was further stirred at 318 K for 15 min. The obtained copper NCs were purified by precipitation upon addition of isopropanol. Herein, glutathione is chosen as a capping agent to stabilize the NCs, which has been widely used in the synthesis of fluorescent Ag and Au NCs.[19,32] Upon addition of diluted $N_2H_4 \cdot H_2O$ to the mixture of glutathione and copper sulphate, the color of the solution changed to light yellow with stirring at 318 K for 15 min, which suggests the formation of Cu NCs. The photography of the as-prepared Cu NCs in aqueous solution is shown in Figure 1. In addition, there is no obvious precipitation formation, which is attributed to the stabilizing effect of glutathione which prevent the NCs agglomeration. Upon UV irradiation (365 nm), Cu NCs show strong red fluorescence (Figure 1) and the quantum yield could reach up to 2.1% using Rodamine 6G as a standard. Moreover, freeze-dried Cu NCs solid also show red luminescence under UV light (Figure S1). In addition, the Cu NCs exhibit a well-defined excitation spectrum centered at 394 nm and emission at 585 nm (Figure 2).

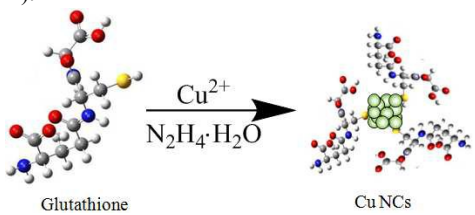

Scheme 1 The formation process of glutathione-directed synthesis of stable and water-soluble red fluorescent Cu NCs.

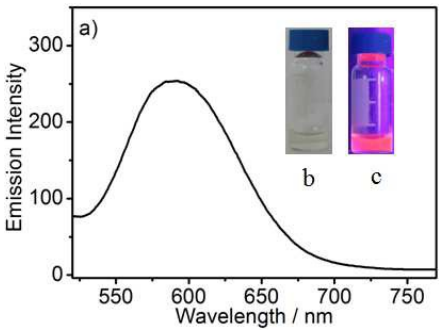

Figure 1 a) The fluorescent spectrum of Cu NCs in aqueous solution at room temperature. The inset images show the photographs of NCs under (b) the natural light and (c) 365 nm UV light.

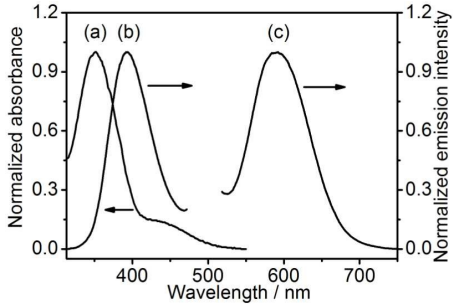

Figure 2 a) The normalized absorbance spectrum of potassium dichromate aqueous solution. b) The normalized excitation spectrum of Cu NCs aqueous solution. c) The normalized emission spectrum of Cu NCs in aqueous solution.

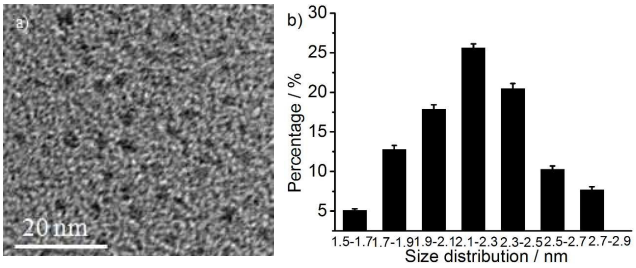

Figure 3 a) Typical TEM image of as-prepared Cu NCs at room temperature; b) Size distribution: the average size was 2.2 ± 0.6 nm.

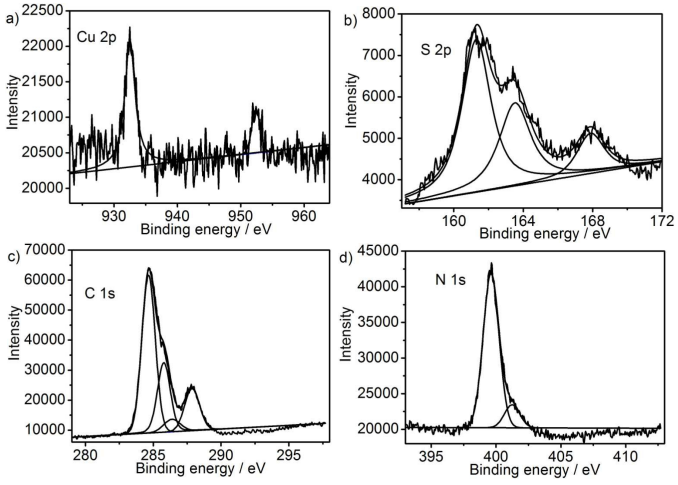

Figure 4 XPS spectra of as-prepared Cu NCs: a) Cu 2p; b) S 2p; c) C 1s; d) N 1s.

The transmission electron microscopy (TEM) image of as-prepared Cu NCs is shown in Figure 3. The average size of the Cu NCs is 2.2 ± 0.6 nm. Moreover, there is no formation of larger size nanoparticles or aggregation, which highlights the unique template effect of glutathione for the preparation of NCs. To further characterize the as-prepared Cu NCs, the oxidation state and elemental composition of Cu NCs were determined by X-ray photoelectron spectroscopy (Figure 4). In the present study, the binding energy of Cu $2p_{3/2}$ was calculated to be 932.5 eV,[33] which is assigned to the binding energy of Cu(0), and a weak peak could be observed at 952.4 eV, which indicates a very minimal presence of Cu(II).[34] The peak at 161.3, 163.5, and 167.9 eV are the characteristic signals of S 2p, which are in accordance with Cu–S, S, and oxidized sulfur, respectively. The binding energy of C1s could be interpreted as having four different components at 287.8 (–COOH), 286.4 ($–CONH_2$), 285.8 (–CH-), 284.6 eV ($–CH_2CH_3$).[35] The N 1s peak at 399.6 and 401.2 eV indicates the presence of –NH and $–NH_3^+$, respectively.[36] On the other hand, the surface chemistry of as-prepared Cu NCs was confirmed by FT-IR spectroscopy. Comparing the FT-IR spectra of NCs and pure glutathione, there was no difference in their spectra, suggesting that Cu NCs would not affect the surface structure of glutathione (Figure S2). The results of photoluminescence, photoluminescence excitation, transmission electron microscopy, X-ray photoelectron spectroscopy, FT-IR spectra confirm that Cu NCs are successfully synthesized.

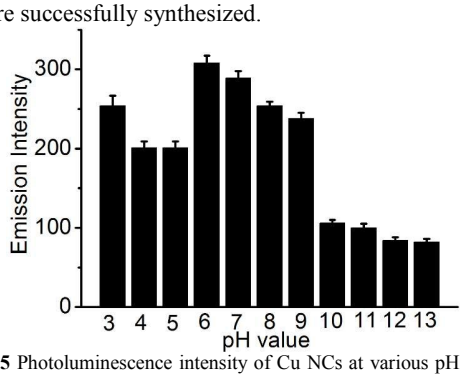

Figure 5 Photoluminescence intensity of Cu NCs at various pH values (room temperature).

Optical responses of fluorescent Cu NCs to pH

To assess the stability of Cu NCs in different pH, optical responses to changes in pH were performed. A series of fluorescent Cu NCs solutions with different pH values ranging from 3 to 13 were prepared, and the fluorescence intensity was measured by using spectrofluorimeter. Significant changes of fluorescence intensity were observed as the pH value varied (Figure 5). As indicated, it is obvious that the emission intensity could reach the maximum value at pH = 6. The emission intensity decreases significantly from pH = 6 to pH = 13 and changes a little from pH = 6 to pH =3. Meanwhile, a red-shift in the emission peak from 580 nm to 591 nm could be observed as the pH value changes from 6 to 3 (Figure S3).

Optical responses of fluorescent Cu NCs to $Cr_2O_7^{2-}$ ion

Glutathione is a naturally occurring and readily available tripeptide with several functional groups including amino and carboxyl groups. The biocompatible glutathione encourages Cu NCs to have good solubility in aqueous solution. Generally speaking, glutathione has good affinity towards metal ions, such as Cu^{2+}, Hg^{2+}, Pb^{2+}, which is important for practical applications in ions detection.[37] However, no obvious cation ions (Na^+, Ba^{2+}, Cd^{2+}, Cu^{2+}, Co^{2+}, Fe^{3+}, Hg^{2+}, Mg^{2+}, Mn^{2+}, Zn^{2+}, Pb^{2+}, Cr^{3+}, Ag^+, Fe^{2+}, Al^{3+}) responses are observed for Cu NCs (Figure 6a).

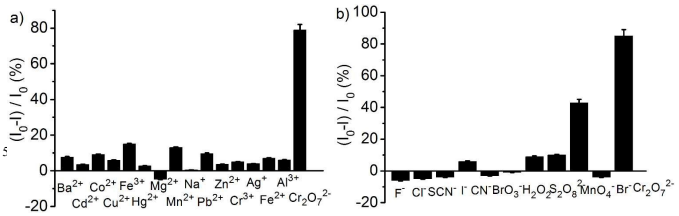

Figure 6 Relative emission intensity $(I_0–I)/I_0$ of as-prepared Cu NCs upon addition of (a) 2.1×10^{-5} mol·L^{-1} of different metal ions and (b) 3.1×10^{-5} mol·L^{-1} of different anion ions. I_0 and I represent the maximum emission intensity of Cu NCs before and after addition of metal or anion ions or hydrogen peroxide.

Interestingly Cu NCs could be used as a probe for the detection of $Cr_2O_7^{2-}$ ion. Upon addition of different amounts of $Cr_2O_7^{2-}$ ion, the emission intensity is gradually quenched with the increase of the concentration of $Cr_2O_7^{2-}$ ion. The emission spectral changes of Cu NCs upon addition of $Cr_2O_7^{2-}$ ion at about 293 K is shown in Figure 7. Moreover, a linear relationship between the logarithm of fluorescence intensity and the concentration of $Cr_2O_7^{2-}$ ion is observed over the range from 0 μmol·L^{-1} to 45 μmol·L^{-1}, which is also shown in Figure 7. Furthermore, the limit of detection is estimated to be 1.5 μmol·L^{-1} (0.16 mg·L^{-1}) in terms of a signal-to-noise of 3.

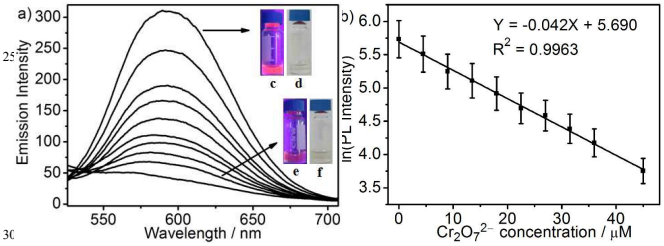

Figure 7 a) Emission spectral changes of Cu NCs in water upon addition of different amounts of $Cr_2O_7^{2-}$ ions (From top to bottom: 0, 4.5, 9, 13.5, 18, 22.5, 27, 31.5, 36, 45 μmol·L^{-1}). b) Linear relationship between the logarithm of emission intensity and the concentration of $Cr_2O_7^{2-}$ ions. The inset images show the photographs of NCs under a 365 nm UV light (c) without and (e) with $Cr_2O_7^{2-}$ ion, under the natural light (d) without and (f) with $Cr_2O_7^{2-}$ ion.

To test the selectivity of Cu NCs towards $Cr_2O_7^{2-}$ ion, other ions including anion ions (F^-, Cl^-, Br^-, I^-, CN^-, BrO_3^-, $S_2O_8^{2-}$, SCN^-, MnO_4^-) and cation ions (Na^+, Ba^{2+}, Cd^{2+}, Cu^{2+}, Co^{2+}, Fe^{3+}, Hg^{2+}, Mg^{2+}, Mn^{2+}, Zn^{2+}, Pb^{2+}, Cr^{3+}, Ag^+, Fe^{2+}, Al^{3+}) together with H_2O_2 are also used for the specificity study of Cu NCs probe. These ions are performed under the same conditions as $Cr_2O_7^{2-}$ ion. The responses of Cu NCs towards these ions manifested by the fluorescence intensity variation are shown in Figure 6. The results indicate that fewer fluorescence intensity changes are observed for these ions relative to $Cr_2O_7^{2-}$ ion and the major interference is MnO_4^- ion, which is purple color and has wide absorption ranging from UV to visible region (Figure S4). These results confirm that our NCs have good selectivity to $Cr_2O_7^{2-}$ ion.

The reasons for the fluorescence quenching of the Cu NCs towards $Cr_2O_7^{2-}$ ion mainly arise from the inner filter effect of $Cr_2O_7^{2-}$ ion, which has been reported in the previous literature.[9] A high efficiency of inner filter effect needs a good spectral overlap between the absorption band of the absorber and the excitation spectrum of the fluorophore. As indicated in Figure 2, excitation spectrum of Cu NCs shows strong emission intensity at 330–470 nm and has good spectral overlap with the absorption spectrum of $Cr_2O_7^{2-}$ ion. Therefore, the increase of the absorption for $Cr_2O_7^{2-}$ ion could be effectively converted to the fluorescence quenching.

As is known to us, Cu NCs have intense fluorescence while Cu(II) only have blue color but have no fluorescence. Upon addition of $K_2Cr_2O_7$ to 45 μmol·L^{-1}, the color of the solution has no obvious change (Figure 7), which suggests that few Cu NCs change into Cu(II). The result could be further supported by X-ray photoelectron spectroscopy (XPS) results of Cu NCs without and with $K_2Cr_2O_7$ (Figure S5), which suggests that the proportionality of Cu(II) in total copper increase from 20% to 35% and have no obvious change, estimated by the integration area plotted in intensity versus binding energy by using XPS spectroscopy. In addition, other oxidant agents including $S_2O_8^{2-}$ and H_2O_2 both does not result in obvious fluorescence quenching (Figure 6b), further suggesting the fluorescence quenching of Cu NCs does not mainly arise from the oxidation of Cu NCs to Cu(II) ion. As contrast, oxidant agent such as MnO_4^- ion results in relative obvious fluorescence quenching. In view of good spectral overlap between the excitation spectrum of Cu NCs and the absorption spectrum of MnO_4^- ion (Figure S4) at 330–400 nm, the reasons for the fluorescence quenching of the Cu NCs towards MnO_4^- ion mainly arise from the inner filter effect of MnO_4^- ion. All the data confirm that fluorescence quenching of Cu NCs upon addition of $K_2Cr_2O_7$ is proposed to be mainly comprised of the inner filter effect of $Cr_2O_7^{2-}$ ion.

Table 1 Recoveries of Cr(VI) ion spiked in tap water, mineral water, and Taihu lake water by Cu NCs with six measuring times of repetition.

	tap water			mineral water		
added Cu^{2+} (μM)	found Cu^{2+} (μM)	Recovery (%)	RSD (%)	found Cu^{2+} (μM)	Recovery (%)	RSD (%)
4.48	4.52	100.9	6.5	4.42	98.7	5.2
17.8	18.2	102.2	4.8	18.3	102.8	5.9
31.9	31.1	97.5	5.1	30.8	96.5	4.1
	Taihu lake water					
added Cu^{2+} (μM)	found Cu^{2+} (μM)	Recovery (%)	RSD (%)			
4.48	4.39	98.0	6.3			
17.8	16.9	94.9	5.6			
31.9	32.8	102.8	5.1			

To further assess the application of Cu NCs in real water, Cu NCs were used as a probe to determine $Cr_2O_7^{2-}$ ion in tap water, mineral water, Taihu lake water spiked with different amounts of $Cr_2O_7^{2-}$ ion. Real water samples were firstly filtered to remove any suspensions. Studies were carried out with nine concentration (0, 4.5, 9, 13.5, 18, 22.5, 27, 31.5, 36 μmol·L^{-1}) spiked in each real water sample. Clearly, the fluorescence intensity gradually decreases with the increase of the amounts of $Cr_2O_7^{2-}$ ion (Figure S5–S7). Moreover, a linear relationship between the logarithm of fluorescence intensity and the concentration of $Cr_2O_7^{2-}$ ion is observed over the range from 0 to 36 μmol·L^{-1} (Figure S6–S8). The result indicates that Cu NCs is highly sensitivity towards $Cr_2O_7^{2-}$ ion. Furthermore, the recovery tests are performed in the three types of samples spiked with a fixed amount of $Cr_2O_7^{2-}$ ion (Table 1), and the relative standard deviations water samples at concentrations of 4.48, 17.8, and 31.9 μmol·L^{-1} are close to 100% (from 94% to 110%), which suggests that the fluorescence method performs well for $Cr_2O_7^{2-}$ ion detection in real water. Although the limit of detection is estimated to be 1.5 μmol·L^{-1} (0.16 mg·L^{-1}) in terms of a signal-to-noise of 3, which is higher than the guideline limit of the World Health Organization for

chromium detection in drinking water (0.04 mg·L^{-1}). However, our method is easy and could detect Cr(VI) ion in water samples without enrichment.

Optical responses of fluorescent Cu NCs to temperature

The obvious temperature dependence of fluorescence intensity of Cu NCs is shown in Figure 8. The intensity decreases by 95% upon the increase of the temperature from 279 K to 323 K. The emission spectra of the as-prepared Cu NCs do not shift with the investigated temperature window. Moreover, a linear relationship between the logarithm of the fluorescence intensity and the temperature is observed. Given this temperature range is larger than the physiological temperature, the temperature probe has promising applications in cell and in vivo temperature sensing. Furthermore, the thermal responses of Cu NCs is reversible upon temperature cycling between 288 K and 313 K for five temperature cycling, and there is a slight temperature hysteresis during heating and cooling processes (Figure S9).

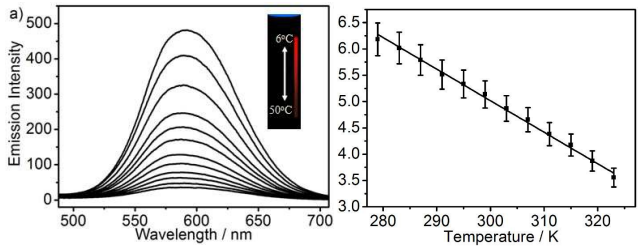

Figure 8 a) Emission spectral changes upon increasing the temperatures from 279 K (top curve) to 323 K (bottom curve). b) Linear relationship between the logarithm of emission intensity and temperatures. The inset image shows a color change model of the temperature gradient.

Herein, we develop one method to modulate the fluorescence intensity by the variation of temperatures in the range 279 K to 323 K. A color change model of the temperature gradient is observed (Figure 8). The top is bright red fluorescence and the bottom is dark red. while the color of the middle part continuously changes from bright red to dark red with the increase of the temperature (inset image of Figure 8). In this case, the temperature could be readily estimated or measured compared with the temperature-dependent Cu NCs chromaticity diagram, and this technique provides a useful tool for the detection of temperature.

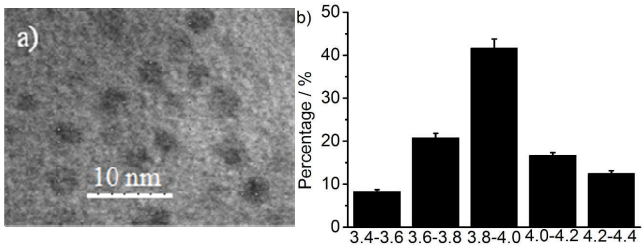

Figure 9 a) The TEM image of Cu NCs in aqueous solution at 318 K. b) Size distribution: the average size was 3.8 ± 0.4 nm.

To further understand fluorescence quenching mechanism on the variation of the temperature, TEM is used to study the temperature-responsive behavior of the NCs. As shown in Figure 9, the average diameters of Cu NCs is about 3.8 nm at 318 K, while the average diameter of Cu NCs at room temperature is about 2.2 nm. Hence, with the increase of the temperature, the aggregation of Cu NCs occurred which caused the obvious fluorescence quenching.[26]

Cellular imaging of fluorescent Cu NCs

The future clinical applications of fluorescent nanomaterials in diagnosis and treatment of cancers or other diseases are dependent on their cytotoxicity eventually. In this reseach, methylthiazolyldiphenyltetrazolium (MTT) assay and apoptosis assay were used to evaluate the cytotoxicity of GSH-Cu NCs and the viability of the HeLa cells. From the results of MTT assay (Figure 10), the viability of the cells still remained above 70% after incubation with GSH-Cu NCs even at the concentration of 80 μg·mL^{-1} for 24 h. Therefore, the result suggested that GSH-Cu NCs had low acute toxicity to HeLa cells.

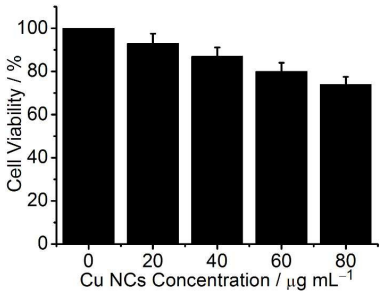

Figure 10 Viability of HeLa cells after 24 h incubation with different concentration of GSH-Cu NCs in the cell medium as determined by a MTT assay.

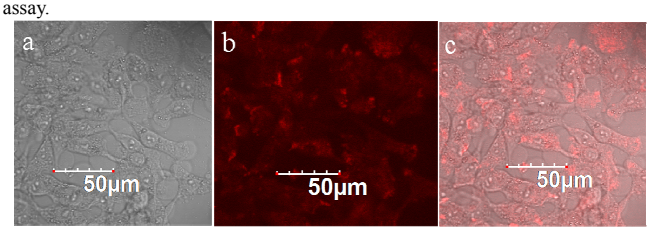

Figure 11 a) Bright field and b) confocal fluorescent and c) overlayed imaging of HeLa cell imaging captured by laser scanning confocal microscopy.

With these advantages including inherited NIR fluorescence, water-solubility, and biocompatibility, as-prepared Cu NCs could be promising candidate for cellular imaging. The HeLa cell internalization and intracellular distribution of Cu NCs were evaluated by confocal laser fluorescence microscopy. Figure 11 revealed the bright field, confocal fluorescence, and overlayed images of the cells incubation with Cu NCs. From the bright field image, we could see the cells incubated with resultant Cu NCs still remain their normal morphology, suggesting the good biocompatibility of Cu NCs at this specific dose and time point. The fluorescence image irradiated by 405 nm showed bright red fluorescence within the HeLa cells that showed the uptake behavior of the cells. It could be seen that the fluorescence signals was mostly distributed in the cytoplasm. The result indicated that the NIR Cu NCs could be used as a probe for optical cellular imaging.

To deeply understand nanothermometry devices for temperature sensing in HeLa cell, the cellular imaging of GSH-Cu NCs at 293 K, 303 K, 313 K was evaluated by confocal fluorescence microscopy. Figure 12 revealed that the confocal fluorescence images of cells incubated with Cu NCs at the concentration of 20 μg/mL for 24 h, whose fluorescence was in the NIR region. In addition, the fluorescence image was greatly quenched with the increase of the temperature. The results indicate that the as-prepared NCs could be used as versatile nanothermometry devices in cellular temperature sensing based on obvious

temperature dependence on the logarithm of fluorescence emission intensity.

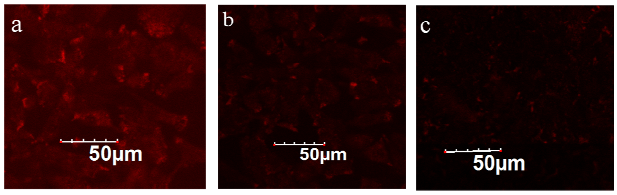

Figure 12 Confocal fluorescent images of HeLa cells incubated with GSH-Cu NCs for 24 h measured at about (a) 293 K; (b) 303 K; (c) 313 K.

Conclusion

In summary, water-soluble and fluorescent active Cu NCs were successfully synthesized by one-step reaction. As-prepared Cu NCs showed red fluorescence with peak maximum at 585 nm and quantum yields up to 2.1% at room temperature. Furthermore, the surface of Cu NCs was protected by glutathione, which made NCs have good solubility and high stability in aqueous solution. The results confirmed that the as-prepared NCs showed excellent sensitivity and high selectivity for $Cr_2O_7^{2-}$ ion based on inner filter effect mechanism in water with a detection limit of 1.5 μM. Moreover, the NCs could be used as probe for determination of $Cr_2O_7^{2-}$ ion in real water samples including tap water, mineral water, and Taihu lake water. In addition, the temperature dependence on the fluorescence emission intensity attributing to aggregation-induced fluorescence quenching mechanism has also been observed and approximately linear in physiological temperature range, which makes the NCs promising candidate in cellular and in vivo temperature sensing. We anticipate that our material will provide new insights for the development of multifunctional nanosensors for ions and temperature.

Acknowledgements

This work was supported by the Health Bureau Foundation of Wuxi City, China (MS201524). We also acknowledge support from Wuxi Center for Disease Control and Prevention, China.

Notes and references

[a]*Wuxi Center for Disease Control and Prevention, Wuxi 214023, P.R. China; E-mail: konglingcan2010@163.com; wxcdclingxia@sina.com*
[b]*Department of Basic Science, Jilin Jianzhu University, Changchun 130118, P. R. China;*

1. Z. Q. Yuan, M. H. Peng, Y. He and E. S. Yeung, *Chem. Commun.*, 2011, **47**, 11981–11983.
2. A. Das, S. Bhattacharya, M. Palaniswamy and J. Angayarkanni, *World J. Microbiol. Biotechnol.*, 2014, **30**, 2315–2324.
3. R. Clarke, L. Connolly, C. Frizzell and C. T. Elliott, *Toxicol. Lett.*, 2015, **238**, 54–64.
4. W. Ji, Y. Wang, I. Tanabe, X. Han, B. Zhao and Y. Ozaki, *Chem. Sci.*, 2015, **6**, 342–348.
5. S. A. Katz and H. Salem, *J. Appl. Toxicol.*, 1993, **13**, 217–224.
6. H. Abdolmohammad-Zadeh and G.H. Sadeghi, *Talanta*, 2012, **94**, 201–208.
7. H. G. Preuss, B. Echard, N. V. Perricone, D. Bagchi, T. Yasmin and S. J. Stohs, *J. Inorg. Biochem.*, 2008, **102**, 1986–1990.
8. G. Bauer, M. A. Neouze and A. Limbeck, *Talanta*, 2013, **103**, 145–152.
9. M. Zheng, Z. Xie, D. Qu, D. Li, P. Du, X. Jing and Z. Sun, *ACS Appl. Mater. Interfaces* 2013, **5**, 13242−13247.
10. G. Kucsko, P. C. Maurer, N. Y. Yao, M. Kubo, H. J. Noh, P. K. Lo, H. Park and M. D. Lukin, *Nature*, 2013, **500**, 54–58.
11. K. Okabe, N. Inada, C. Gota, Y. Harada, T. Funatsu and S. Uchiyama, *Nat. Commun.*, 2012, **3**, 705–713.
12. P. R. N. Childs, J. R. Greenwood, C. A. Long, *Rev. Sci. Instrum.*, 2000, **71**, 2959–2978.
13. S. W. Allison, G. T. Gillies, *Rev. Sci. Instrum.*, 1997, **68**, 2615–2650.
14. G. Kwak, S. Fukao, M. Fujiki, T. Sakaguchi and T. Masuda, *Chem. Mater.*, 2006, **18**, 2081–2085.
15. R. Z. Liang, R. Tian, W. Y. Shi, Z. H. Liu, D. P. Yan, M. Wei, D. G. Evans and X. Duan, *Chem. Commun.*, 2013, **49**, 969–971.
16. D. Yan, J. Lu, J. Ma, M. Wei, D. G. Evans and X. Duan, *Angew. Chem. Int. Ed.*, 2011, **50**, 720–723.
17. Y. Hiruta, M. Shimamura, M. Matsuura, Y. Maekawa, T. Funatsu, Y. Suzuki, E. Ayano, T. Okano and H. Kanazawa, *ACS Macro Lett.*, 2014, **3**, 281–285.
18. Y. Liu, J. Hu, Y. Li, H. P. Wei, X. S. Li, X. H. Zhang, S. M. Chen and X. Q. Chen, *Talanta*, 2015, **134**, 16–23.
19. L. Kong, W. Liu, X. Chu, Y. Yao, P. Zhu, X. Ling, *RSC Adv.*, 2015, **5**, 80530–80535.
20. M. Valden, X. Lai and D. W. Goodman, *Science*, 1998, **281**,1647–1650.
21. R. Lghanian, J. J. Storhoff, R. C. Mucic, R. L. Letsinger, C. A. Mirkin, *Science*, 1997, **277**, 1078–1081.
22. J. Yu, S. Choi and R. M. Dickson, *Angew. Chem. Int. Ed.*, 2009, **48**, 318–320.
23. T. H. Lee, J. I. Gonzalez, J. Zheng and R. M. Dickson, *Acc. Chem. Res.*, 2005, **38**, 534–541.
24. C. Wang, L. Xu, H. Cheng, Q. Lin and Chi Zhang, *Nanoscale*, 2014, **6**, 1775–1781.
25. T. Li, L. B. Zhang, J. Ai, S. J. Dong and E. K. Wang, *ACS Nano*, 2011, **5**, 6334–6338.
26. C. Wang, H. Cheng, Y. Sun, Z. Xu, H. Lin, Q. Lin and C. Zhang, *Microchim. Acta*, 2015, **182**, 695–701.
27. Z. Wu, M. Wang, J. Yang, X. Zheng, W. Cai, G. Meng, H. Qian, H. Wang and R. Jin, *small*, 2012, **8**, 2028–2035.
28. J. Zhang, L. Tu, S. Zhao, G. Liu, Y. Wang, Y. Wang and Z. Yue, *Biosens. Bioelectron.*, 2015, **67**, 296–302.
29. C. Wang, Z. Xu, H. Cheng, H. Lin, M. G. Humphrey and C. Zhang, *Carbon*, 2015, **82**, 87–95.
30. H. Kim, B. I. Lee and S. H. Byeon, *Chem. Commun.,* 2015, **51**, 725–728.
31. H. Cheng, C. Wang, Z. Xu, H. Lin and C. Zhang, *RSC Adv.*, 2015, **5**, 20–26.
32. X. Zhang, F.-G. Wu, P. Liu, N. Gu and Z. Chen, *Small*, 2014, **10**, 5170–5177.
33. X. Yuan, Z. T. Luo, Q. B. Zhang, X. H. Zhang, Y. G. Zheng, J. Y. Lee and J. P. Xie, *ACS Nano*, 2011, **5**, 8800–8808.
34. C. Vazquez-Vazquez, M. Banobre-Lopez, A. Mitra, M. A. Lopez-Quintela and J. Rivas, *Langmuir*, 2009, **25**, 8208–8216.
35. F. Xia, L. Feng, S. T. Wang, T. L. Sun, W. L. Song, W. H. Jiang and L. Jiang, *Adv. Mater.*, 2006, **18**, 432–436.
36. E. S. Shibu and T. Pradeep, *Chem. Mater.*, 2011, **23**, 989–999.
37. C. Wang, Y. Wang, L. Xu, X. Shi, X. Li, X. Xu, H. Sun, B. Yang and Q. Lin, *Small*, 2013, **9**, 413–420.

TOC

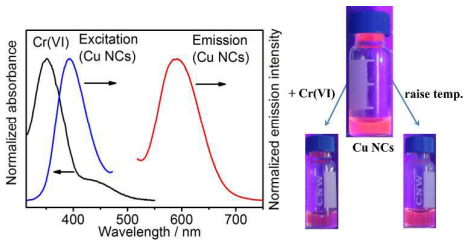

Highly red luminescent GSH-Cu nanoclusters were synthesized and could be used as nanosensors for Cr(VI) ion and temperature.